NASA TM X-55668

ON THE IMPEDANCE OF A SATELLITE BORNE VLF ELECTRIC FIELD ANTENNA

BY

T. L. AGGSON AND C. A. KAPETANAKOS

AUGUST 1966

NASA ———— GODDARD SPACE FLIGHT CENTER ————
GREENBELT, MARYLAND

ON THE IMPEDANCE OF A SATELLITE BORNE

VLF ELECTRIC FIELD ANTENNA

by

T. L. Aggson and C. A. Kapetanakos

NASA-Goddard Space Flight Center

Greenbelt, Maryland

ON THE IMPEDANCE OF A SATELLITE BORNE

VLF ELECTRIC FIELD ANTENNA

Abstract: The source impedance of a satellite borne VLF antenna is calculated using probe theory. Numerical examples of the impedance are given for typical plasma parameters for a short cylindrical antenna. It is shown that at these frequencies the resistive component dominates the imaginary component along both ionospheric and magnetospheric satellite orbits. This result is used to re-examine the interpretation in terms of electrostatic waves to explain the VLF noise observed by the satellite 1964-45A. It is shown that if a VLF antenna is monitored with a charge sensitive amplifier, the output signal is proportional to the product of the ambient signal level and the plasma density. The sustained noise enhancements observed on the 1964-45A satellite are thus attributed to changes in the antenna impedance along the satellite orbit rather than from changes in the ambient plasma noise level.

Introduction

The VLF electric field experiment aboard the 1964-45A satellite consisted of a short cylindrical antenna and four RMS voltmeters which monitored the AC voltages induced on the antenna in four frequency channels from 1.7-kc/s to 14.5-kc/s [Scarf et al., 1964]. The authors reported that background VLF electric field strength rarely fell below one mV/m in the ionosphere and the lower magnetosphere. In addition, sustained noise enhancements were observed on the night side of the orbit which correlated with specific L shells and with the precipitation of energetic electrons. The experimenters interpreted these noise enhancements as direct evidence of electrostatic ion waves in those regions where the noise enhancements were observed.

These experimental results are of considerable interest from the view point of plasma dynamics as well as geophysics. We have considered it worthwhile to consider in some detail the possibility that the observed noise enhancements were not field oscillations in the local plasma (i.e., geophysical phenomena) but might instead simply represent variations in the antenna impedance with changes in the ambient plasma parameters.

The Resistive Component of the Source Impedance

Following the analysis of Mlodonsky and Garriott [1962] we will assume

that at VLF frequencies the undisturbed plasma acts as an almost perfect

conductor. In this case, which will be justified numerically later, the an-

tenna impedance is determined primarily by the sheath impedance. Con-

sider a short cylindrical antenna like that of the 1964-45A satellite as shown

in Figure 1. The antenna will attain an equilibrium potential, ϕ, which is

given by the solution of the integral equation

$$\int \vec{J}_e \, (\phi) \cdot \vec{dS} = \int \vec{J}_+ \, (\phi) \cdot \vec{dS} + \int \vec{J}_p \, (\phi) \cdot \vec{dS} + I \tag{1}$$

where $J_e \, (\phi)$ is the electron current, $J_+ \, (\phi)$ is the ion current, $J_p \, (\phi)$ is the

photo-emission current, and I is the current drawn from the antenna by the

electrical loading of the receiver. Other charging effects such as secondary

emission will be neglected. Equation (1) represents the condition of equilib-

rium. This condition will be valid in time varying electric fields with fre-

quencies less than the inverse of the relaxation constant τ^{-1} of the plasma

immersed antenna as will be discussed later.

If a potential gradient exists over the dimensions of the antenna, or al-

ternately if the antenna is moving in a magnetic field, the net current into a

2

small surface of the antenna will not necessarily be zero since the plasma potential will be a function of the position $\vec{r}$ of the surface element dS. In equilibrium, however, the total current to the antenna must again be zero.

$$\int \vec{J}_e (\vec{r}, \phi) \cdot d\vec{S} = \int \vec{J}_+ (\vec{r}, \phi) \cdot d\vec{S} + \int \vec{J}_p (\vec{r}, \phi) \cdot d\vec{S} + I \qquad (2)$$

If we assume that the electron distribution in the plasma is essentially Maxwellian and also that the potential of the antenna is negative, the electron current can be treated analytically as

$$\vec{J}_e (\vec{r}, \phi_0) = \vec{J}_{eo} \exp \left\{ \frac{e \left[\phi_0 + (\vec{E} + \vec{V} \times \vec{B}) \cdot \vec{r} \right]}{KT} \right\} \qquad (3)$$

Here ϕ_0 is defined as the potential of the antenna with respect to the plasma potential at the origin of the coordinate system (see Figure 1a), $\vec{J}_{eo}$ is the electron random current density, $\vec{V}$ is the velocity of the satellite, and $\vec{B}$ is the magnetic field strength. The electric field used to derive equation (3) was assumed to be constant over the dimensions of the antenna, i.e., the antenna length is taken to be short compared to the wavelength.

Combining equations (2) and (3) and integrating gives

$$\phi_0 = -\frac{KT}{e} \ln \frac{2\pi J_{eo} \, a \, KT \, d \left[\exp \frac{e(\vec{E} + \vec{V} \times \vec{B}) \cdot \vec{d}}{KT} - 1\right]}{e(\vec{E} + \vec{V} \times \vec{B}) \cdot \vec{d} \left[\int \vec{J}_+ \cdot d\vec{S} + \int \vec{J}_p \cdot d\vec{S} + I\right]} \qquad (4)$$

where a is the antenna radius and d is the antenna length. Equation (4) can be differentiated to yield the following expressions for the voltage gain and the source impedance of the antenna:

Voltage Gain: $$\frac{\partial \phi_0}{\partial E} = \frac{\vec{E} \cdot \vec{d}}{E} \left[\frac{KT}{e(\vec{E} + \vec{V} \times \vec{B}) \cdot \vec{d}} - \frac{1}{1 - \exp\left[-\frac{e(\vec{E} + \vec{V} \times \vec{B}) \cdot \vec{d}}{KT}\right]}\right] + \frac{\frac{KT}{e} \frac{d}{dE} \int \vec{J}_+ \cdot d\vec{S}}{\int \vec{J}_+ \cdot d\vec{S} + \int \vec{J}_p \cdot d\vec{S} + I} \qquad (5)$$

Source Impedance (Rs): $$\frac{\partial \phi_0}{\partial I} = \frac{KT}{e} \frac{1}{\left[\int \vec{J}_+ \cdot d\vec{S} + \int \vec{J}_p \cdot d\vec{S} + I - \frac{KT}{e} \frac{\partial}{\partial \phi_0} \int \vec{J}_+ \cdot d\vec{S}\right]} \qquad (6)$$

For short antennas $e(\vec{E} + \vec{V} \times \vec{B}) \cdot \vec{d} < KT$ and the voltage gain can be approximated by an expansion of the first term of equation (5) as

$$\frac{\partial \phi_0}{\partial E} = -\frac{\vec{E} \cdot \vec{d}}{2E} \left[1 + \frac{1}{6} \frac{e(\vec{E} + \vec{V} \times \vec{B}) \cdot \vec{d}}{KT} + \cdots\right] \qquad (7)$$

4

The second term is a small correction due to focusing effects. When the potential is positive, the following simple empirical expression for the photoelectric current can be derived which agrees well with the experimental results of Hinteregger [1959] for energies below 1.5 volts:

$$\vec{J}_p\left(\phi^+\right) = \vec{J}_{po} \, \exp\left[-\frac{11.8\,\phi_0^+}{h\nu}\right] \tag{8}$$

where $\vec{J}_{po}$ is the photoelectric current density with no applied electric field and $h\nu$ is a constant equal to 6.2 ev.

Following the same procedure as in the case of negative potential, it is readily proved that

$$\phi_0^+ = \frac{h\nu}{11.8} \, \ln \frac{2\pi a \, dJ_{po}\left[1 - \exp\left\{-\frac{11.8}{h\nu}(\vec{E}+\vec{V}\times\vec{B})\cdot\vec{d}\right\}\right]}{\frac{11.8(\vec{E}+\vec{V}\times\vec{B})\cdot\vec{d}}{h\nu}\left[\int\vec{J}_e\cdot d\vec{S} - \int\vec{J}_+\cdot d\vec{S} - I\right]} \tag{9}$$

Equation (9) can be differentiated with respect to the electric field to yield the following expression for the voltage gain of the antenna:

$$\tag{10}$$

$$\frac{\partial\phi_0^+}{\partial E} = \frac{\vec{E}\cdot\vec{d}}{E}\left[\frac{1}{\exp\left\{\frac{11.8}{h\nu}(\vec{E}+\vec{V}\times\vec{B})\cdot\vec{d}\right\}-1} - \frac{h\nu}{11.8(\vec{E}+\vec{V}\times\vec{B})\cdot\vec{d}}\right] - \frac{h\nu}{11.8}\frac{\frac{d}{dE}\left[\int\vec{J}_e\cdot d\vec{S}-\int\vec{J}_+\cdot d\vec{S}\right]}{\left[\int\vec{J}_e\cdot d\vec{S}-\int\vec{J}_+\cdot d\vec{S}-I\right]}$$

5

Using the approximation $\frac{11.8}{h\nu} (\vec{E} + \vec{V} \times \vec{B}) \cdot \vec{d} < 1$, the above equation can be

again approximated by an expansion of the first term on the right

$$\frac{\partial \phi_0^+}{\partial E} = - \frac{\vec{E} \cdot \vec{d}}{2E} \left[1 - \frac{1}{6} \frac{11.8}{h\nu} (\vec{E} + \vec{V} \times \vec{B}) \cdot \vec{d} + \cdots \right] \qquad (11)$$

The source impedance is obtained by differentiating equation (9) with re-

spect to current drawn from the antenna by the electrical loading of the

receiver

$$\frac{\partial \phi_0^+}{\partial I} = \frac{h\nu}{11.8} \frac{1}{\left[\int \vec{J}_e \cdot \vec{dS} - \int \vec{J}_+ \cdot \vec{dS} - I + \frac{h\nu}{11.8} \frac{\partial}{\partial \phi_0^+} \left\{ \int \vec{J}_e \cdot \vec{dS} - \int \vec{J}_+ \cdot \vec{dS} \right\} \right]} \qquad (12)$$

The voltage gain, equations (7) and (11) represents the response of an

unloaded antenna with respect to the plasma potential at the origin to

an external electric field. The actual AC voltage measured by a satellite-

borne receiver will be larger than this amount because of the variation of

the satellite ground potential with respect to the origin. This effect can be

roughly approximated by replacing the antenna length $\vec{d}$ in equation (7) and (11)

by an effective antenna length $\vec{d}_e = \vec{d} + \vec{t}$ where $\vec{t}$ represents the extent of

the satellite along the direction of the vector $\vec{d}$ (see Figure 1a). Also it should

be pointed out that Equations (7) and (11) indicate that the voltage gain should be somewhat sensitive to the antenna orientation with respect to the vector $\vec{V} \times \vec{B}$.

Equations (6), (7), (11) and (12) are valid for time varying electric fields with periods longer than an equilibrium charging time τ. This characteristic relaxation time is given roughly by the relation

$$\tau = R_s C_s$$

where C_s is the antenna capacity which includes the sheath corrections. In addition equations (6), (7), (11), and (12) are strictly valid only at frequencies below the electron plasma frequency since the treatment given here neglects collective effects in the plasma and the effect introduced by the transit time of the electrons across the sheath. The treatment of such effects is beyond the scope of this discussion. This restriction does not limit the present investigation which is concerned with satellite borne VLF antennas since the plasma frequency in the magnetosphere is in general greater than 100 kc/s.

The Antenna Capacity

It was suggested by Storey [1963] and Whale [1964] that the capacity of a plasma immersed cylindrical antenna might be approximated by that of the co-axial capacitor formed by the antenna and the boundary of the plasma sheath, i.e.,

$$C = 2\pi \epsilon_0 \frac{d}{\ln \frac{\lambda + a}{a}}$$

where λ is the sheath thickness, a is the antenna radius, d is the antenna length, and ϵ_0 is the permittivity of free space.

The above expression is not in general true since it diverges for zero potential. A more general expression can be derived by assuming a charge distribution in the sheath like that of Figure 1b, where $a + \lambda + \alpha\lambda_D$ is the distance at which the space charge becomes zero, λ_D is the Debye length, and α is a constant of the order of unity.

The charge inside a cylinder of radius r and length d is given by

$$q(r) = 2\pi d \int_a^r \rho(r) \, r \, dr$$

where $\rho(r)$ is the charge distribution. The total charge can be calculated from the relation

$$q(\lambda) = 2\pi\, d \int_{a}^{a+\lambda+\alpha\lambda_D} \rho(r)\, r\, dr \tag{13}$$

Using Gauss's theorem and $\vec{E} = -\nabla\phi$ the potential on the antenna is obtained

$$\phi_0 = \frac{1}{2\pi\, \epsilon_0\, d} \int_{a}^{a+\lambda+\alpha\lambda_D} \frac{\left[q(\lambda) - q(r)\right]}{r}\, dr \tag{14}$$

The capacity of the antenna can conveniently be defined as

$$C = \frac{dq(\lambda)}{d\phi_0(\lambda)} = \frac{dq(\lambda)/d\lambda}{d\phi_0/d\lambda} \tag{15}$$

Differentiating equation (14) and substituting into (15) we can obtain a simple expression for the capacity

$$C = \frac{2\pi\, \epsilon_0\, d}{\ln \dfrac{a + \lambda + \alpha\lambda_D}{a}} \tag{16}$$

9

Note that the above derivation does not require a knowledge of the exact nature of the charge distribution; only the distance $\lambda + a\lambda_D$ is required. The total charge inside the sheath can be found after integration of (13) between the limits a and a + λ by assuming a constant charge density $n_e e$ shown in Figure 1b. The result is

$$q(\lambda) = \pi d\, n_e\, e\, \left[(\lambda + a)^2 - a^2\right] \tag{17}$$

Combining equations (14) and (17) we can find the value of λ from the expression

$$\phi_0 = \frac{n_e e}{2\epsilon_0} \left\{ (a + \lambda)^2 \ln \frac{a + \lambda + a\lambda_D}{a} - \frac{1}{2} \left[(a + \lambda + a\lambda_D)^2 - a^2 \right] \right\} \tag{18}$$

when the value of ϕ_0 is known.

The above treatment of antenna capacity and sheath thickness does not include the effects of the satellite wake and of the antenna ground plane.

It should be noted that since the plasma parameters enter only into the log term of the antenna capacity the antenna capacity should not vary appreciably as a function of the satellite plasma environment. In

contra-distinction the resistive impedance of the antenna is a much stronger

function of the plasma parameters varying roughly as $R_s \sim \dfrac{KT}{n_e}$.

Numerical Calculations

The ion current to the antenna when the potential on it is negative can

be calculated using the following expression, [Orsak et. al., 1965]

$$J_+ \left(\phi_0\right) = e \left(\frac{KT}{2\pi m_i}\right)^{1/2} n_+ \Psi\sigma \tag{19}$$

where: Ψ is an ion current factor due to the accelerating potential ϕ_0 (see

appendix) and σ is an ion current factor due to satellite velocity (see appendix).

To calculate the Ψ factor, the floating potential is needed. An approx-

imate value of it is given by

$$\phi_0 = \frac{KT}{e} \ln \frac{I_{eo}}{I_{+R}}$$

where I_{eo} is the electron random current and I_{+R} is the ion ram current.

The sheath thickness can be obtained from equation (18), using this calculated value of ϕ_0. Inserting ϕ_0 and λ in the equation (A-1), the Ψ factor is determined.

The σ factor can be calculated from the known ion velocity, if the satellite velocity is given. For roughly circular orbits

$$V \simeq \frac{0.79 \cdot 10^6}{\sqrt{R/R_0}} \text{ cm/sec}$$

where

R = radius vector

R_0 = earth radius

Wave effects will reduce the ion current somewhat.

The photo emission current can be estimated from the experimental results of Hinteregger [1959]:

$$\int \vec{J}_{po} \cdot \vec{dS} = 3.9 \times 10^{-9} S_{\perp s} \text{ [Negative potential]} \tag{20}$$

12

where

$$S_{\perp s} = 2ad \text{ for the cylindrical antenna.}$$

Shadowing will of course reduce this current. Since the photoelectric current does not change appreciably with altitude as long as the potential on the antenna remains negative and since the electron and ion current decreases with increasing altitude, it is expected that the potential on the floating antenna will become zero in a specific altitude. This occurs at $R/R_0 = 2.6$ which can be derived by setting $\phi_0 = 0$ in equation (1) and using equations (19) and (20) for the ion and photoelectric current respectively.

In the case of positive potential the electron current is given by

$$J_e\left(\phi_0^+\right) = e\left(\frac{KT}{2\pi m_e}\right)^{1/2} n_e \Psi$$

The Ψ factor, similar to the previous case, is due to the accelerating potential (see Appendix). In this case, however, the contribution from the motion of satellite can be neglected since the electron thermal velocity is much greater than the satellite velocity.

While the ion current could be calculated from the expression [Kanal, 1964]

$$J_+\left(\phi_0^+\right) = e\left(\frac{KT}{2\pi m_i}\right)^{1/2} n_+ \exp\left\{-\left(\frac{e\phi_0^+}{KT} + \gamma^2\right)\right\}$$

$$\cdot \sum_{n=0}^{\infty} \frac{(2n+1)!\,\gamma}{(n!)^2\, 2^{2n}\left(\frac{e\phi_0^+}{KT}\right)^{n/2}} \; I_n\left[2\gamma\left(\frac{2\phi_0^+}{KT}\right)^{1/2}\right]$$

(here $\gamma^2 = \dfrac{V^2 m_i}{2KT}$, V is the satellite velocity and I_n is the modified Bessel function of the nth order), this is not necessary for the most part since its maximum value is only a few percent of the photoelectron current and therefore can be omitted without introducing a considerable error.

The value of ϕ_0^+ which is necessary for the computation of the Ψ factor can be approximated by the expression

$$\phi_0^+ = \frac{1}{1.9} \ln \frac{J_{eo} - J_{+o}}{J_{po}}$$

while the sheath thickness is given again from equation (18)

14

In order to give numerical examples of the antenna impedance, typical values of the plasma ambient plasma parameters n and T are needed. A useful graphical summary of the plasma conditions in the ionosphere as given by Bourdeau [1965] and Johnson [1962] are shown in Figures 2a and 2b. Estimates of the thermal plasma parameters in the magnetosphere are slightly less well founded at present. Figure 3 shows an average of several orbits of the ion trap measurements of IMP-II [Serbu and Maier, 1966] and one orbit of IMP-I measurements. Calculated values of the resistive portion of the source impedance of an antenna of 1 cm diameter and 100 cm length as a function of altitude are shown in Figure 4 for the ionosphere and Figure 5 for the magnetosphere. These graphs were calculated using equation (6) for negative potential, equation (12) for positive potentials, and the plasma parameters given in Figures (2) and (3). The axis of the antenna was taken as perpendicular to the solar vector, perpendicular to the satellite velocity vector, and perpendicular to the $\vec{V} \times \vec{B}$ vector. It can be seen from these graphs that the resistive portion of the impedance varies considerably with altitude. Values for the geometry chosen vary from Kilo-ohms in the F-layer to tens of Meg-ohms in the outer magnetosphere.

Values of the capacity of an antenna of similar dimensions were calculated from equation (16) and are shown as a function of altitude for the ionosphere in Figure (6) and for the magnetosphere in Figure (7). The

antenna capacity is much less dependent on altitude varying from about 9 pf minimum in the outer magnetosphere to 55 pf maximum in the daytime F-layer.

The above calculations for the antenna impedance are appropriate to a satellite-borne antenna. The resistive component of an antenna aboard a sounding rocket near apogee will be an order of magnitude larger since the ion ram current will be much less. It should also be pointed out that these calculations are for an isolated antenna at the floating potential. By biasing electron current from the antenna into the satellite the resistive impedance can be considerably reduced [Storey, 1963].

It is important to compare the resistive source impedance with the capacity impedance. Since these impedances act electrically in parallel on the antenna [Mlodonsky and Garriott, 1962] the resistive impedance will dominate at frequencies below a value f_0 given by the expression

$$R_s = \frac{1}{2n \, f_0 \, C_s}$$

Values of this transition frequency f_0 are given in Figure 8 for the ionosphere and in Figure 9 for the magnetosphere. It can be seen from these curves that the resistive impedance of a satellite-borne antenna

16

dominates the capacitive impedance at VLF frequencies in both the iono-
sphere and in the lower portions magnetosphere.

The transition frequency f_0 is also equal to the upper limit of the
validity of the derivation of the resistive impedance, equation (6) and (12),
since above this frequency the antenna cannot reach the assumed equilibrium
condition.

It is important to justify the neglect of the bulk impedance of the plasma
if we wish to apply the calculated sheath impedances directly to the in-
terpretation of experimental data. The bulk conductivity of the plasma is
extremely anisotropic due to the magnetic field being a fair conductor along
the field vector and a good insulator perpendicular to it. The conductivity
along the field vector is given by the Lorentz conductivity

$$S = \omega_p^2 \epsilon_0 \frac{\nu_m - i\omega}{\nu_m^2 + \omega^2}$$

where ω_p is the plasma frequency and ν_m is the collision frequency for
momentum transfer of the electrons. Since the collision frequency is con-
siderably less than the signal frequency at VLF frequencies along most
satellite orbits, the bulk conductivity as given above is mostly inductive

17

[Storey, 1963]. One can estimate the frequency domain where the sheath impedance dominates the bulk impedance as follows

$$\frac{1}{R_s} + \omega C_s \ll \frac{\omega_p^2 \epsilon_0 d}{\omega} \qquad (21)$$

For VLF frequencies it has been numerically shown that

$$\frac{1}{R_s} \gg \omega C_s \qquad (22)$$

Using this result and the approximation $C_s \simeq \epsilon_0 d$ equation (21) reduces to

$$\frac{\omega}{R_s C_s} \ll \omega_p^2 \qquad (23)$$

From (22) and (23) we have a frequency domain where the sheath impedance dominates the bulk impedance

$$\omega \ll \omega_p \qquad (24)$$

18

This frequency domain includes the VLF phenomena at satellite altitudes as already noted.

Antenna Pre-Amplifier Considerations

From the above considerations we can conclude that although the voltage gain, equations (7) and (11), of a satellite-borne VLF antenna is to a first approximation independent of the ambient plasma parameters, the antenna impedance is a strong function of these parameters. Of the two satellite VLF electric field intensity experiments reported to date, The experiment of Storey [1963] utilizes a voltage sensitive preamplifier as shown schematically in Figure 10a. Modern semi-conductor technology allows the design of such an amplifier with a resistive input impedance of the order of hundreds of Meg-ohms. Thus this type of preamplifier allows the measurement of VLF signals with receiver gain independent of the ambient plasma conditions.

On the other hand, the VLF experiment on the 1964-45A satellite utilized a charge sensitive pre-amplifier [Scarf et. al., 1965] as is illustrated schematically in Figure 10b neglecting the sheath capacity. The output signal of such an amplifier is proportional to the time integral of the input

$$V_{out} \propto \int \frac{V_s}{R_s} \, dt \qquad (25)$$

where V_s would be the signal induced on the antenna if it was unloaded by the amplifier and R_s is the sheath impedance. At a particular frequency f_n in the Fourier domain this expression reduces to the form

$$\left(V_{out}\right)_{fn} \propto \frac{\left(V_s\right)_{fn}}{R_s}$$

at the altitudes of this experiment (300 km – 4000 km) the source impedance is determined primarily by the ion ram current

$$R_s \propto \frac{KT}{e} \frac{1}{en_e \, VS_{\perp}}$$

Thus, to a first approximation, this experiment apparently measured a quantity proportional to the <u>product</u> of the ambient electric field intensity and the plasma density

$$V_{out} \propto \frac{E_f \, n_e}{KT} \qquad (26)$$

20

Alternate Interpretation of the Measurements of Scarf et al.

In view of the above analysis of the actual physical quantity measured in the 1964-45A satellite electric field experiment we feel that a reinterpretation of the geophysics involved is in order. As mentioned earlier the RMS voltages measured indicated a slowly varying background level on the daytime apogee half of the orbits with sustained signal enhancements at 1.7-kc/s on the nighttime perigee portion with some general correlation with specific L shells and with the precipitation of energetic electrons. The authors [Scarf et. al., 1965] interpreted these signal enhancements as direct evidence of electrostatic ion waves in the ambient plasma since they could not conceive of an alternate explanation of the correlation of the signal enhancement with specific L shells and energetic electron fluxes.

The point to be made here is that there is an alternate explanation of the observed correlation of these signal enhancements with either specific L shells or energetic particles in terms of the variation of the antenna-amplifier response with the ambient plasma density as given by equation (26). The magnetic control of the plasma density in the upper ionosphere was observed with a probe aboard the Ariel I satellite [Sayers et. al., 1963] and confirmed with the first top side sounder satellite [King et. al., 1964]. In addition, observations with both the Ariel and Aloutte I satellite suggest that energetic particles should be considered as an ionization source of the

21

F-region electron density [Bordeau, 1965]. More recently Sharp [1966] has found troughs and enhancements in the plasma density as a function of latitude by means of a ion trap carried aboard an earth-oriented circular satellite at roughly 300 km altitude. The total variation in plasma density during one orbit was larger than a factor of one hundred. Converting these changes in plasma density to changes in antenna amplifier response via equation (26) allows one a simple explanation of the apparent noise enhancement measured aboard the 1964-45A satellite in terms of changes in antenna impedance.

In addition to the variations in the relative noise levels in the ionospheric plasma, the absolute magnitude of the noise is of great interest. Since the analysis given in this paper indicates that the 1964-45A electric field experiment monitored a quantity which was physically different from what it was calibrated for, we feel that the absolute magnitudes of the noise levels reported are perhaps also questionable.

Conclusions

I. The resistive component of the source impedance of a satellite-borne antenna dominates the capacitive component at VLF frequencies in both the ionosphere and the lower magnetosphere.

II. The antenna impedance varies considerably as a function of altitude.

III. The experimental results of the VLF electric field experiment [Scarf et. al., 1965] flown aboard the 1964-45A satellite can perhaps be re-interpreted. In particular the correlation of the apparent noise enhancements observed with specific L shells and with the observation of precipitating energetic electrons can be interpreted as representing changes in the antenna impedance because of the charge sensitive characteristics of the amplifier used rather than representing an observation of ion-acoustic waves.

APPENDIX

The ion current density to the antenna, for negative potential and assuming thermal equilibrium of ions, is given by [Orsak et. al., 1965]

$$J_+\left(\phi_0\right) \;=\; J_{+o}\,\Psi\sigma$$

where:

$$J_{+o} \;=\; \frac{e}{4}\left(\frac{2KT}{\pi m_i}\right)^{1/2} n_+ \;=\; \text{ion random current}$$

n_+ = ion density

m_i = ion mass

$$\Psi \;=\; \frac{a+\lambda}{a}\,\mathrm{erf}\left[\frac{a^2\,e\phi_0}{(\lambda+2a)\,\lambda KT}\right]^{1/2} + \exp\frac{e\phi_0}{KT}\,\mathrm{erfc}\left[\frac{(a+\lambda)^2\,e\phi_0}{(\lambda+2a)\,\lambda\,KT}\right]^{1/2} \quad\text{(A-1)}$$

a = antenna radius

λ = sheath thickness

T = ion temperature

The σ factor represents the contribution to ion current from the satellite motion. Assuming that the velocity vector is perpendicular to the antenna axis it can be expressed as

$$\sigma = \frac{2}{\pi} \, \nu \, E\left(\nu, \, \frac{\pi}{2}\right)$$

where

$$\nu = \exp\left(-\frac{x^2}{2}\right) + x\left(\frac{\pi}{2}\right)^{1/2} \left[2 \int_{-\infty}^{x} \phi(x) \, dx - 1\right]$$

$$\phi(x) = (2\pi)^{-1/2} \exp\left(-\frac{x^2}{2}\right)$$

and

$$x = V\left(\frac{m_i}{KT}\right)^{1/2}$$

and E is a complete elliptic integral of the second kind.

FIGURE CAPTIONS

Figure 1a   Antenna geometry

Figure 1b   Postulated charge distribution inside the sheath

Figure 2a   Typical electron density for the ionosphere as summarized
by Bordeau [1965]

Figure 2b   Typical electron temperature for the ionosphere [Bordeau,
1965]

Figure 3   Plasma parameters for the magnetosphere [Serbu and
Maier, 1966]

Figure 4   Resistive impedance of a short cylindrical antenna (0.5
radius; 100 cm length) in the ionosphere. The antenna axis
assumed perpendicular to the direction of motion and
$T_e = T_i$, $n_e = n_i$.

Figure 5   Resistive impedance of a short cylindrical antenna (0.5
radius; 100 cm length) in magnetosphere. The antenna axis
assumed perpendicular to velocity vector and the solar
vector. Also $T_e = T_i$ and $n_e = n_i$.

Figure 6   Capacity of a short cylindrical antenna (0.5 radius; 100

cm length) in the ionosphere. The antenna axis assumed

perpendicular to the direction of motion. The cut-off

parameter a is taken as unity for these calculations.

Figure 7   Capacity of a short cylindrical antenna (0.5 cm radius; 100

cm length) in magnetosphere. The velocity vector assumed

perpendicular to the antenna axis and the solar vector and

the cut-off parameter a is taken as unity.

Figure 8   Transition frequency for a satellite-borne VLF antenna in

the ionosphere. The region to the left of curves represents

the domain where the resistive part of the impedance domi-

nates the capacitive part of the impedance.

Figure 9   Transition frequency for a satellite-borne VLF antenna in

the magnetosphere. The region to the left of the curve

represents the domain where R_s dominates of R_c.

Figure 10   Preamplifier schematics. V_s represents the unloaded source

voltage and R_s represents the sheath impedance. The ca-

pacitor in the charge sensitive amplifier may be alternately

returned to ground rather than the output terminal with no

appreciable change in the transfer functions over the fre-

quency region where the amplifier is charge sensitive, $R_s C > \frac{1}{\omega}$.

REFERENCES

Bordeau, R. E., Research Within the Ionosphere, Science, 148 (3670), 585-594, 1965.

Hinteregger, H. E., K. R. Damon, and L. A. Hall, Analysis of Photoelectrons from Solar Extreme Ultraviolet, J. Geophys Res., 64 (8), 961-969, 1959.

Johnson, F. S., Atmospheric Structure, Astronautics, 7 (8), 54-61, 1962.

Kanal, M., Theory of Current Collection of Moving Cylindrical Probes, J. Appl. Phys., 35 (6), 1697-1703, 1964.

King, J. W., P. A. Smith, D. Eccles, H. Helm, topside sounder satellite observations which indicate possible interactions between energetic particles and the earth's atmosphere, Proc. of the 5th Intern. Sp. Sc. Symposium, Florence, 1964, Space Research, Vol. 5, pp. 214-215, 1965.

Mlodnosky, R. F., and O. K. Garriott, The V. L. F. admittance of a dipole in the lower-ionosphere, Proc. Intern. Conf. Ionosphere, London, 1962, pp. 484-491, Institute of Physics and the Physical Society, London, 1963.

Orsak, L. E., L. H. Rorden, G. B. Carpenter, and B. P. Ficklin, VLF Propagation and noise in the ionosphere observed by sounding rocket, Stanford Res. Inst. Final Report, January 1965.

Sayers, J., P. Rothwell, and J. Wager, Field-aligned strata in the ionization above the ionospheric F$_2$ layer, Nature, 198, 230-233, 1963.

Scarf, F. L., G. M. Crook, and R. W. Fredricks, Preliminary report on detection of electrostatic ion waves in the magnetosphere, J. Geophys. Res., 70 (13), 3045-3060, 1965.

Serbu, G. P., E. J. R. Maier, Low energy electrons measured on IMP-II, NASA Rept. X-615-66-92, Goddard Space Flight Center, Greenbelt, Maryland, January 1966.

Sharp, G. N., Midlatitude trough in the night ionosphere, J. Geophys. Res., 71 (5), 1345-1346, 1966.

Storey, L. R. O., The design of an electric dipole antenna for VLF reception within the ionosphere, Tech. Rept. 308 TC, Centre National D'Etudes des Te'le'communications, Department Te'le'commande, July 1963.

Whale, H. A., Ion Sheath effects near antennas radiating within the ionosphere, J. Geophys. Res., 69 (3), 447-455, 1964.
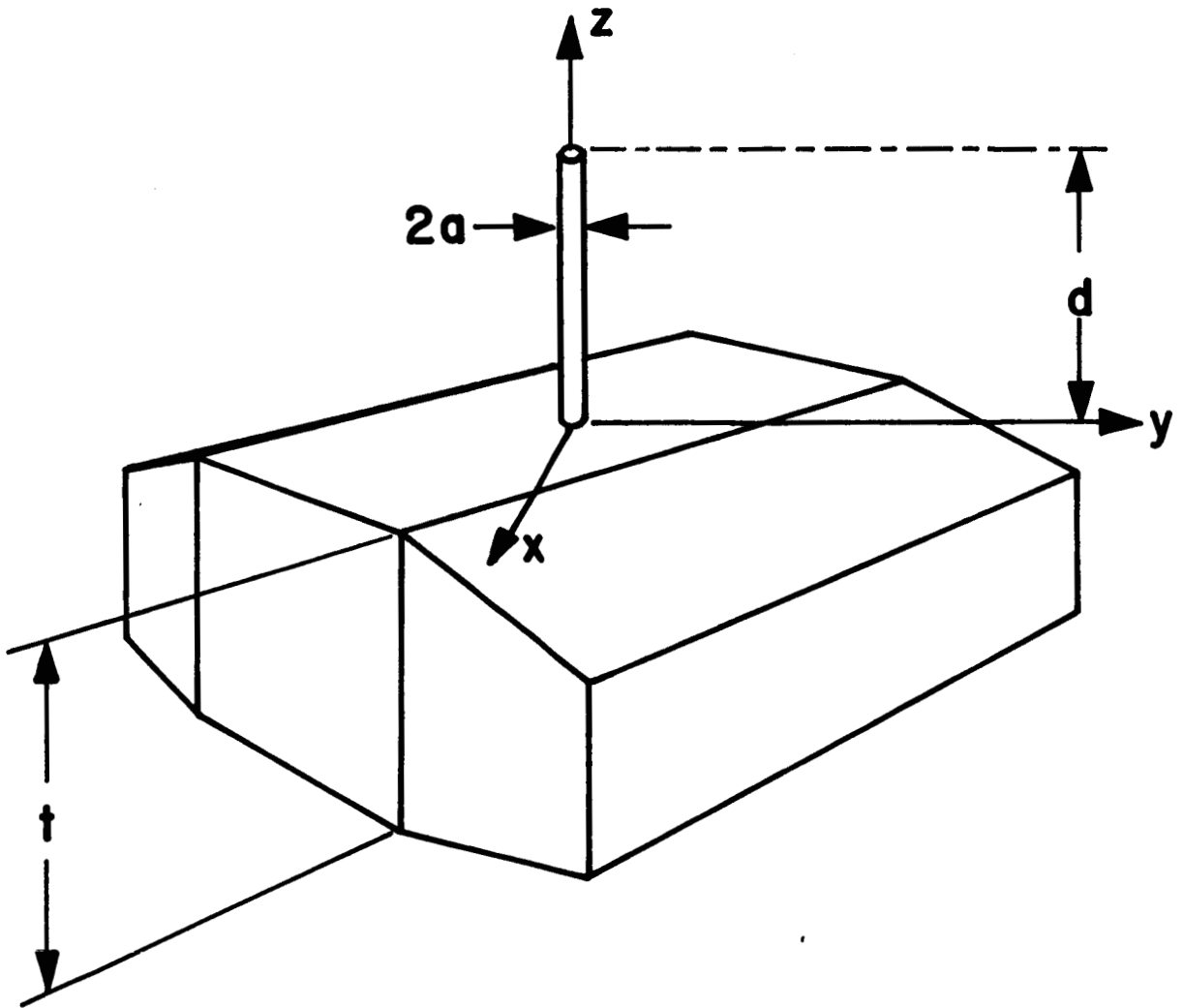
ANTENNA GEOMETRY
Figure 1a
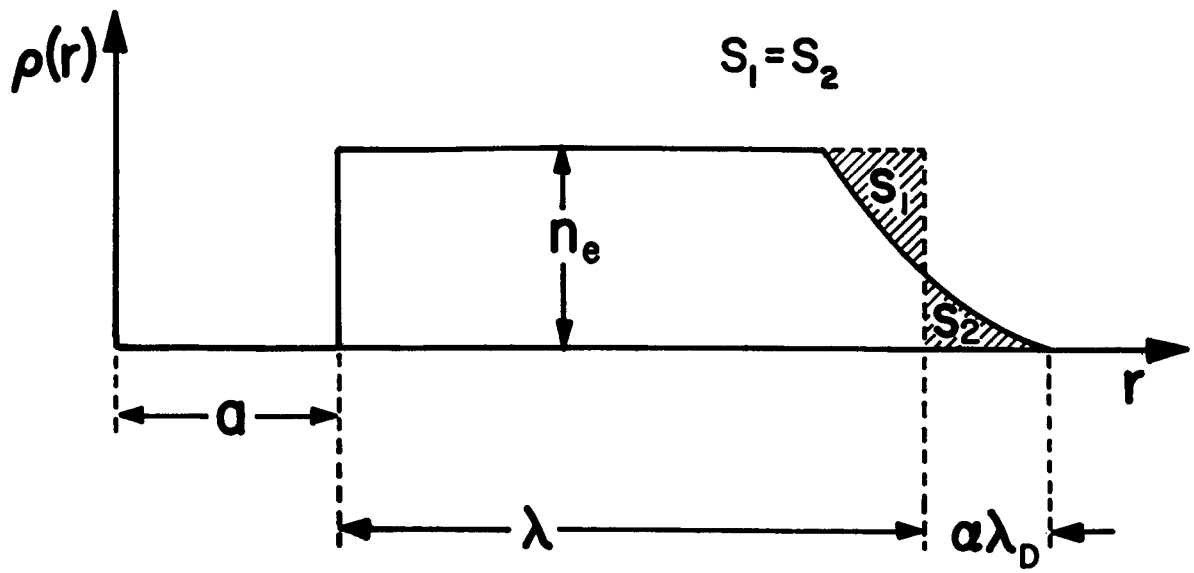
Figure 1b
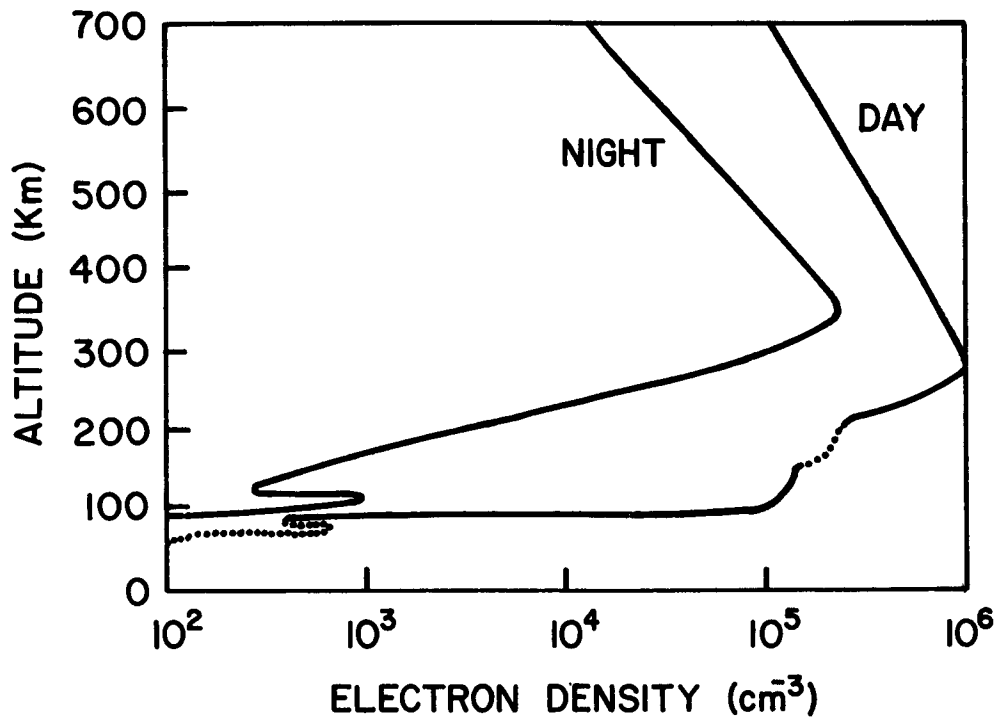
Figure 2a
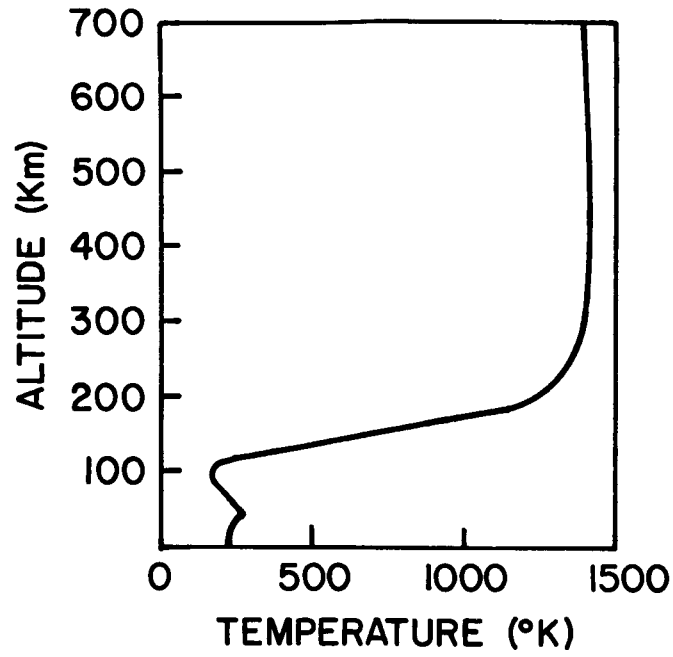
Figure 2b

Figure 3

Figure 4

36
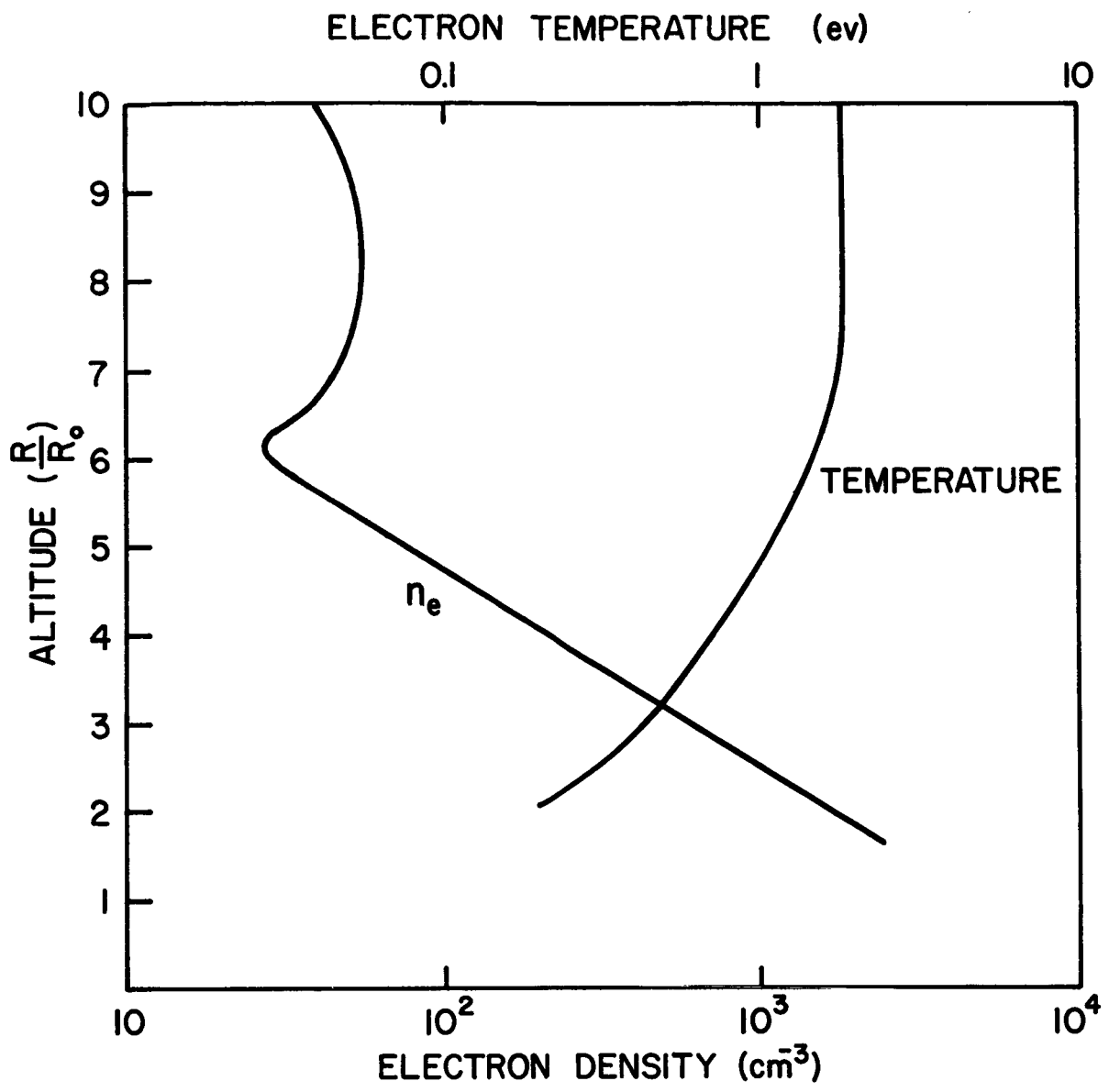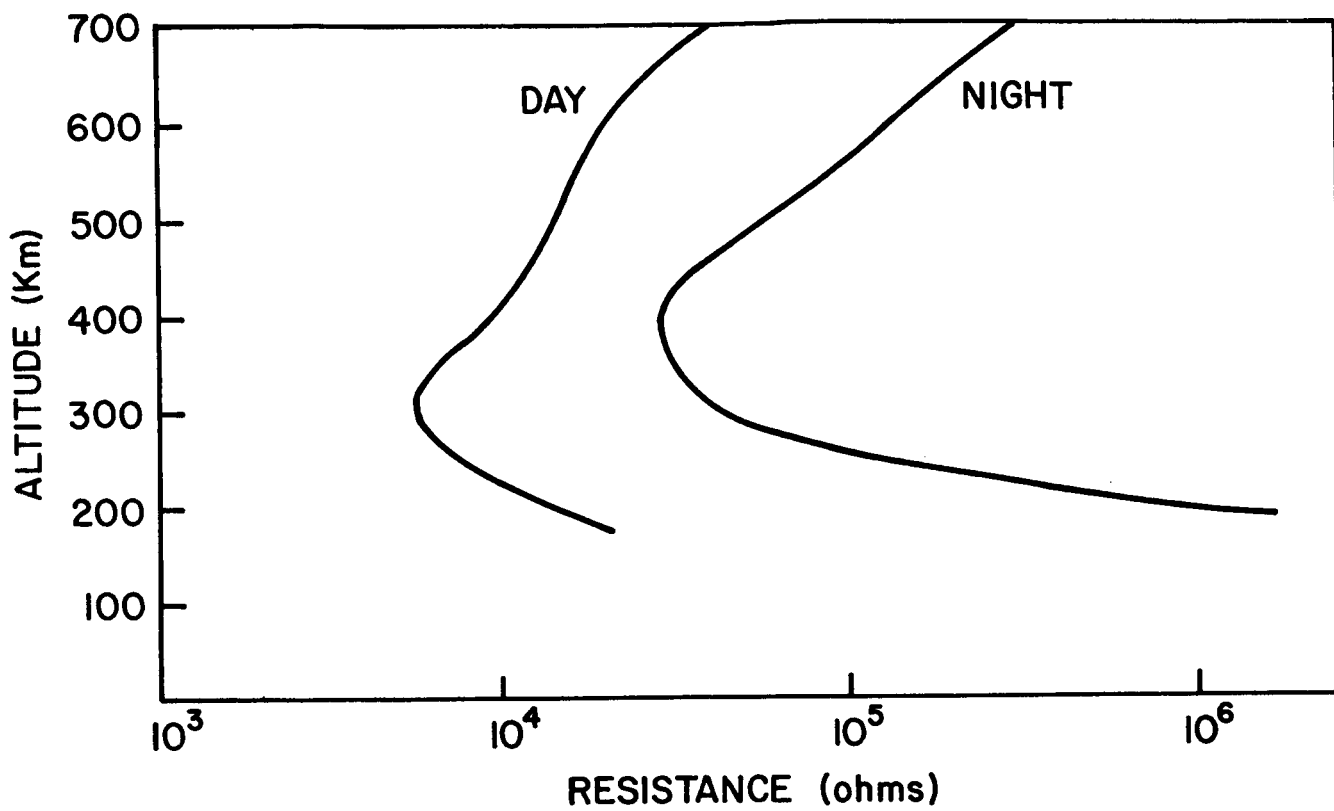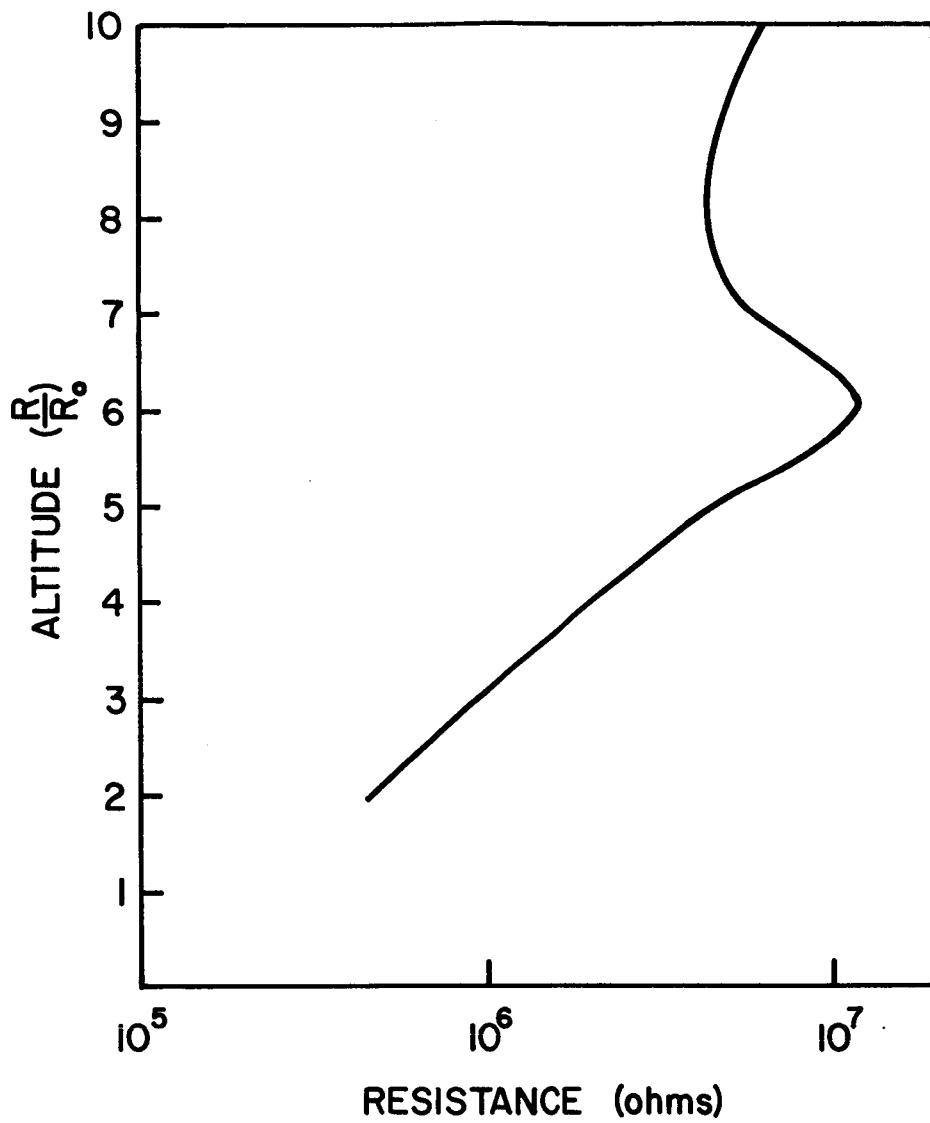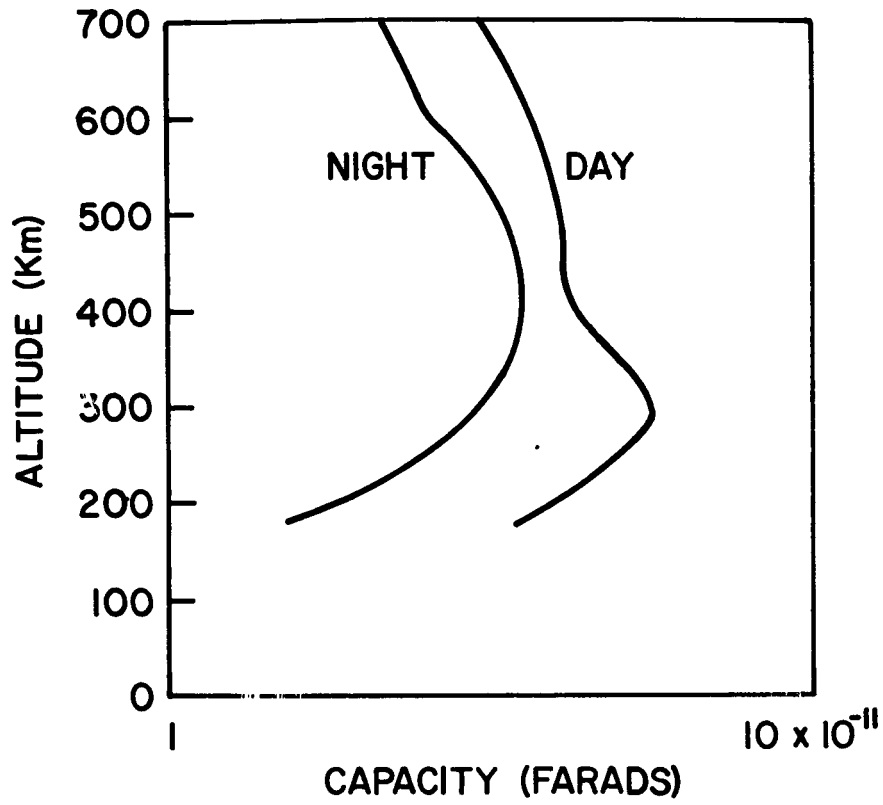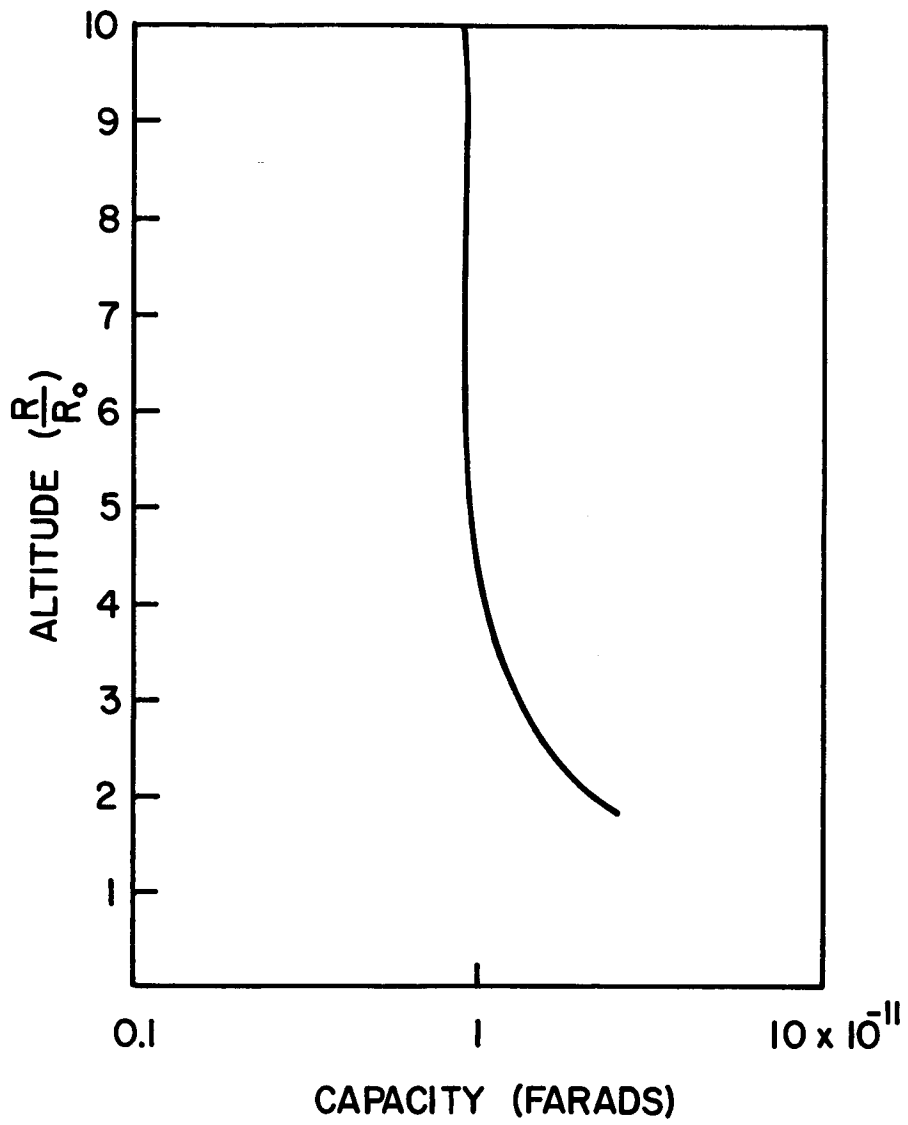
Figure 5

Figure 6

Figure 7

Figure 8

Figure 9

41
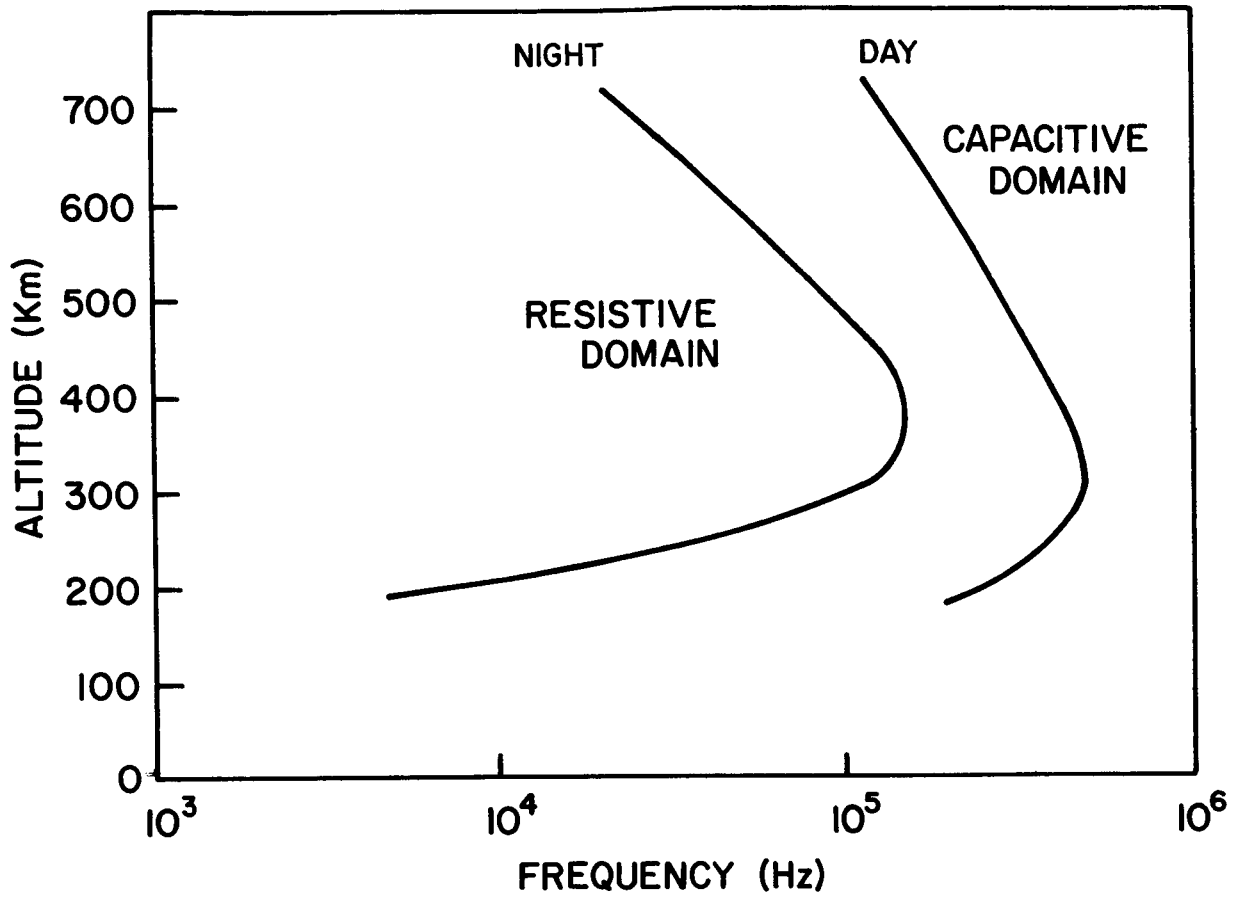
a) Voltage Sensitive Amplifier

$V_{out} \propto V_s$
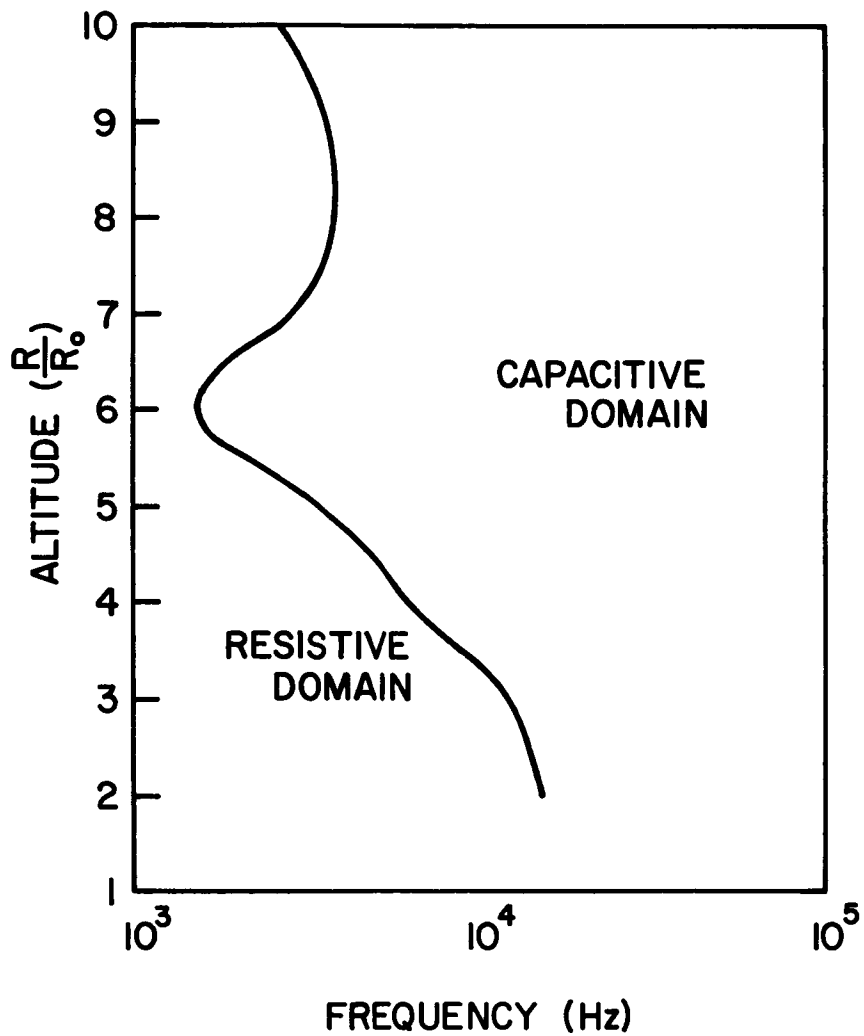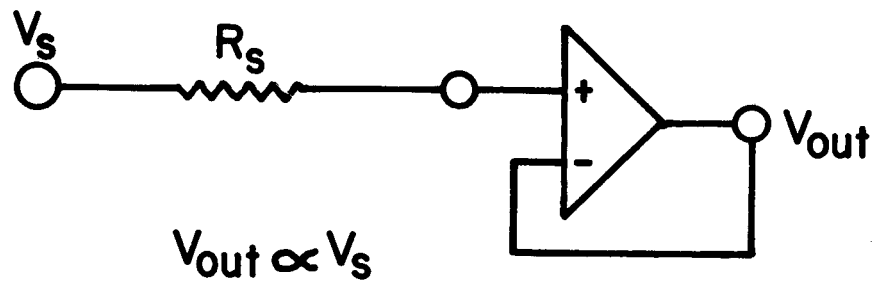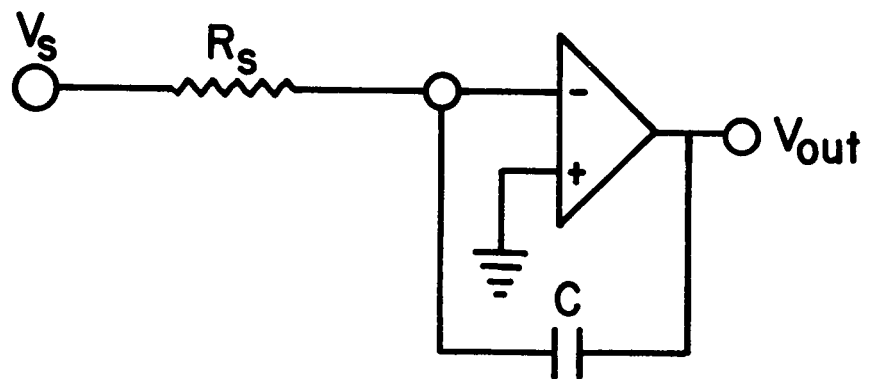
b) Charge Sensitive Amplifier

$$V_{out} \propto \int \frac{V_s}{R_s} dt : \text{Real Domain}$$

$$(V_{out})_{fn} \propto \frac{(V_s)_{fn}}{R_s} : \text{Fourier Domain}$$

PREAMPLIFIER SCHEMATICS
Figure 10